Olefin Copolymerization via Controlled Radical Polymerization: Copolymerization of Methyl Methacrylate and 1-Octene

Rajan Venkatesh and Bert Klumperman*

Dutch Polymer Institute, Department of Polymer Chemistry, Eindhoven University of Technology, Den Dolech 2, P.O.Box 513, 5600 MB Eindhoven, The Netherlands

Received August 19, 2003; Revised Manuscript Received December 22, 2003

ABSTRACT: The atom transfer radical (co)polymerization (ATRP) of methyl methacrylate (MMA) with 1-octene was investigated. Well controlled homopolymer of MMA was obtained with 2,2,2-trichoroethanol (TCE) and *p*-toluenesulfonyl chloride (pTsCl), although, uncontrolled copolymerization occurred when pTsCl was employed in the presence of higher mole percent of 1-octene in the monomer feed. Well-controlled copolymers constituting almost 20 mol % of 1-octene were obtained using TCE as initiator. Narrow molar mass distributions (MMDs) were obtained in the ATRP experiments**.** The comparable free radical (co)polymerizations (FRP) resulted in broad MMDs. Increasing the mol % of the olefin in the monomer feed, led to an increase in the level of incorporation of the olefin in the copolymer, at the expense of the overall percent conversion. The formation of the copolymer was established using matrix assisted laser desorption/ionization−time-of-flight−mass spectrometry (MALDI−TOF−MS). Evident from the MALDI−TOF−MS spectra was that most polymer chains contained at least one 1-octene unit. The glass transition temperature of the copolymer was 16 °C lower than that for the homopolymer of MMA. Block copolymer was synthesized and further characterized using gradient polymer elution chromatography (GPEC). The shift in the retention time between the macroinitiator and the formed block, clearly indicated the existence of the block copolymer structure and also confirmed the high macroinitiator efficiency.

Introduction

Copolymers of α-olefins with polar monomers with various architectures remain an ultimate goal in polyolefin engineering, since, of the many permutations available for modifying the properties of the polymers, the incorporation of functional groups into an otherwise nonpolar material is substantial.[1,2]

Pioneering work in this field of olefin copolymerization with polar monomers, has been carried out in the area of metal-catalyzed insertion polymerization. The Brookhart Pd-based diimine catalyst[3] has been shown to copolymerize ethylene and higher α-olefins with acrylates and vinyl ketones.[4] Other late transition-metal-based complexes are also known to tolerate the presence of polar functional groups.[5] Block copolymers of ethylene with acrylates and methacrylates using group 4 metals are known.[6] Recently published reviews encompass the work in this field.[7] Although catalyst systems showing excellent behavior for both olefins and polar monomers do exist, due to differences in the reactivity between the two monomers, still energetically compatible mechanisms must be satisfied in order for true (random) copolymerization of these two types of monomer to occur. Very recent developments, from Novak[8] were indicative of the fact that, olefins could be copolymerized with vinyl monomers via a free radical mechanism. This was followed up by a publication detailing the copolymerization of methyl acrylate (MA) with 1-alkenes under atom transfer radical polymerization (ATRP) conditions.[9]

The present paper deals with the copolymerization of methyl methacrylate (MMA) [a monomer having a high equilibrium constant (K_{eq}) under ATRP conditions and a lower rate constant for propagation (k_p) as compared to the acrylates] with 1-alkenes (in particular, 1-octene). Because of MMA's low k_p, coupled with the fact that α-olefins undergo degradative chain transfer of allylic hydrogens,[10] the copolymerization reaction is highly unlikely. A heterogeneous transition metal/ligand system is employed for the ATR polymerizations. Results of the successfully controlled copolymerization and characterization by spectroscopic techniques are presented. A comparison of the ATRP results with conventional free radical polymerization using azo initiators is made. The choice/influence of initiator during the copolymerization in the presence of the olefin will be highlighted. Furthermore, the synthesized P[(MMA)-*co*-(1-octene)] is used as a macroinitiator for block polymer synthesis. The macroinitiator efficiency is monitored using gradient polymer elution chromatography (GPEC).

Scheme 1. General Scheme for ATRP

Initiation

$$R{-}X + Cu^{I}X/L \underset{k_d^0}{\overset{k_a^0}{\rightleftharpoons}} R^* + Cu^{II}X_2/L \quad (1)$$

$$R^* + M \xrightarrow{k_p^0} P_1^* \quad (2)$$

Propagation

$$P_n{-}X + Cu^{I}X/L \underset{k_d}{\overset{k_a}{\rightleftharpoons}} P_n^* + Cu^{II}X_2/L \quad (3)$$

$$P_n^* + M \xrightarrow{k_p} P_{n+1}^* \quad (4)$$

Solubilization

$$Cu^{I}X/L_{sol} \underset{k^{I}_{sol}}{\overset{k^{I}_{insol}}{\rightleftharpoons}} Cu^{I}X/L_{insol} \quad (5)$$

$$Cu^{II}X_2/L_{sol} \underset{k^{II}_{sol}}{\overset{k^{II}_{insol}}{\rightleftharpoons}} Cu^{II}X_2/L_{insol} \quad (6)$$

Termination

$$P_m^* + P_n^* \xrightarrow{k_{tD}^{m,n}} D_m^{H} + D_n^{=} \quad (7)$$

$$P_m^* + P_n^* \xrightarrow{k_{tC}^{m,n}} D_{m+n} \quad (8)$$

10.1021/ma035231f CCC: $27.50
Published on Web 01/30/2004

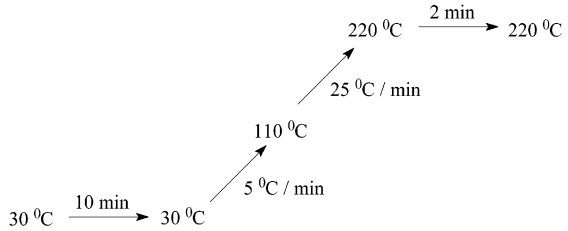

Figure 1. GC temperature gradient.

ATRP[11,12] is one of the techniques employed to obtain living (or controlled) radical polymerization. In copper-mediated ATRP, the carbon−halogen bond of an alkyl halide (RX) is reversibly cleaved by a $Cu^{I}X$/ligand system resulting in a radical (R*) and $Cu^{II}X_2$/ligand (deactivator). The radical will mainly either reversibly deactivate, add monomer or irreversibly terminate (Scheme 1), where R* and P_n* are radicals from initiator and polymer, respectively, R−X and P_n−X are halogen terminated initiator and polymer chains with halide end group, M is monomer, D^{H} and $D^{=}$ are the dead polymer chain with a hydrogen and vinyl-end group respectively and D_{m+n} are the dead chains formed as a result of termination via combination. Rate coefficients for activation (k_a), deactivation (k_d), propagation (k_p), solubilization (k_{sol}), insolubilization (k_{insol}), chain length dependent termination via combination ($k_{tC}^{m,n}$) and chain length dependent termination via disproportionation ($k_{tD}^{m,n}$).

Experimental Section

Materials. Methyl methacrylate (MMA, Merck, 99+%) and 1-octene (Aldrich, 98%) were distilled and stored over molecular sieves at −15 °C. *p*-Xylene (Aldrich, 99+% HPLC grade) was stored over molecular sieves and used without further purification. *N*,*N*,*N*′,*N*″,*N*″-Pentamethyldiethylenetriamine (PMDETA, Aldrich, 99%), ethyl-2-bromoisobutyrate (EBriB, Aldrich, 98%), 2,2,2-trichloroethanol (TCE, Aldrich, 99%), *p*-toluenesulfonyl chloride (pTsCl, Aldrich, 99%), copper(I) bromide (CuBr, Aldrich, 98%), copper(II) bromide ($CuBr_2$, Aldrich, 99%), copper(I) chloride (CuCl, Aldrich, 98%), copper(II) chloride ($CuCl_2$, Aldrich, 98%), aluminum oxide (activated, basic, for column chromatography, 50−200 μm), tetrahydrofuran (THF, Aldrich, AR), and 1,4-dioxane (Aldrich, AR) were used as supplied. α,α′-Azobis(isobutyronitrile) (AIBN, Merck, >98%) was recrystallized twice from methanol before use. 1,1′-Azobis(cyclohexane-1-carbonitrile) (Vazo 88, Dupont, >98%) was used as procured.

Analysis and Measurements. Determination of Conversion and MMD. Monomer conversion was determined from the concentration of the residual monomer measured via gas chromatography (GC), a Hewlett-Packard (HP-5890) GC, equipped with an AT-Wax capillary column (30 m × 0.53 mm × 10 μm) was used. *p*-Xylene was employed as the internal reference. The GC temperature gradient used is given in Figure 1.

Molar mass (MM) and molar mass distributions (MMD) were measured by size exclusion chromatography (SEC), at ambient temperature using a Waters GPC equipped with a Waters model 510 pump, a model 410 differential refractometer (40 °C), a Waters WISP 712 autoinjector (50 μL injection volume), a PL gel (5 μm particles) 50 × 7.5 mm guard column, and a set of two mixed-bed columns (Mixed-C, Polymer Laboratories, 300 × 7.5 mm, 5 μm bead size, 40 °C). THF was used as the eluent at a flow rate of 1.0 mL/min. Calibration was carried out using narrow MMD polystyrene (PS) standards ranging from 600 to 7×10^6 g/mol. The molecular weights were calculated using the universal calibration principle and Mark−Houwink parameters [13] [PMMA, $K = 9.55 \times 10^{-5}$ dL/g, $a = 0.719$; PS, $K = 1.14 \times 10^{-4}$ dL/g, $a = 0.716$]. The molecular weights were calculated relative to PMMA homopolymer. Data acquisition and processing were performed using Waters Millenium 32 software.

Table 1. Linear Binary Gradient Used for GPEC

step	time (min)	$\Phi_{heptane}$	Φ_{THF}	flow (mL/min)
1	initial	1	0	0.5
2	15	0	1	1.0
3	25	0	1	0.5
4	30	1	0	0.5

GPEC Analysis. GPEC measurements were carried out on an Alliance Waters 2690 separation module with a Waters 2487 dual λ absorbance detector and a PL-EMD 960 ELSD detector (Nitrogen flow 5.0 mL/min, temperature 70 °C). A Zorbax silica 5 μm column (4.6 mm × 150 mm, Dupont Chromatography) was used at 40 °C. The gradient employed is detailed in Table 1. The column was reset at the end of the gradient to initial conditions between 25 and 30 min. HPLC grade solvents were obtained from BioSolve. A Varian 9010 solvent delivery system was used to maintain a stable flow rate of the eluents. Dilute polymer solutions were made in THF (10 mg/mL) and a sample of 10 μL was used for analysis. Chromatograms were analyzed using the Millennium 32 software version 3.05.

The eluent compositions are given in volume fraction (Φ).

MALDI—TOF—MS. Measurements were performed on a Voyager-DE STR (Applied Biosystems, Framingham, MA) instrument equipped with a 337 nm nitrogen laser. Positive-ion spectra were acquired in reflector mode. DCTB (*trans*-2-[3-(4-*tert*-butylphenyl)-2-methyl-2-propenylidene]malononitrile) was chosen as the matrix. Potassium trifluoracetate (Aldrich, 98%) was added as the cationic ionization agent. The matrix was dissolved in THF at a concentration of 40 mg/mL. Potassium trifluoracetate was added to THF at a concentration of 1 mg/mL. The dissolved polymer concentration in THF was approximately 1 mg/mL. In a typical MALDI experiment, the matrix, salt, and polymer solutions were premixed in the following ratio: 5 μL of sample:5 μL of matrix:0.5 μL of salt. Approximately 0.5 μL of the obtained mixture was hand spotted on the target plate. For each spectrum, 1000 laser shots were accumulated.

DSC. Scans were done on a TA Instruments Advanced Q1000 standard differential scanning calorimeter. The instrument was calibrated according to the standard procedure suggested by TA Instruments based on indium, sapphire, and standard polyethylene. The standards were all supplied by TA Instruments. The DSC temperature gradient used was, 20 to 150 °C at a rate of 10 °C/min. The step change in the heat flow during the second heating run was considered for the glass transition temperature determination. The T_g was calculated at the inflection (inflection is the portion of the curve between the first and third tangents with the steepest slope).

Synthetic Procedures. Copolymerization of MMA and 1-Octene. A typical polymerization was carried out in a 50 mL three-neck round-bottom flask. *p*-Xylene (11.05 g), MMA (2.42 g, 2.42×10^{-2} mol), 1-octene (2.71 g, 2.42×10^{-2} mol) CuCl (0.037 g, 3.7×10^{-4} mol), and $CuCl_2$ (0.003 g, 2×10^{-5} mol) were accurately weighed and transferred to the flask. The ligand, PMDETA (0.07 g, 4×10^{-4} mol) was then added. After the reaction mixture was bubbled with argon for 30 min, the flask was immersed in a thermostated oil bath kept at 90 °C and stirred for 10 min. A light green, slightly heterogeneous system was then obtained. The initiator, TCE (0.15 g, 1.0×10^{-3} mol) was added slowly via a degassed syringe. The reactions were carried out under a flowing argon atmosphere. Samples were withdrawn at suitable time periods throughout the polymerization. A predetermined amount of the sample was transferred immediately after withdrawing into a GC vial and diluted with 1,4-dioxane, so as to determine the monomer conversion using GC. The remaining sample was diluted with THF, passed through a column of aluminum oxide prior to SEC and MALDI−TOF−MS measurements.

Bulk Polymerization of MMA (Chain Transfer Experiments). Solutions of varying [MMA]/[1-octene] ratios were prepared (Table 3). The initiator (Vazo 88) ([initiator] = 10

Table 2. Homopolymerization of MMA (ATRP)

entry	initiator	reacn time (min)	fractl convn	M_n (g/mol)	PDI
1	pTsCl[a,b]	230	0.74	7.1×10^3	1.08
2	TCE[a,b]	180	0.45	2.8×10^3	1.25

[a] Targeted M_n = 5000 g/mol; [initiator]:[CuCl]:[PMDETA] = 1:0.5:0.5, reaction temperature = 90 °C. [b] Volume {*p*-xylene}/{monomer} = 1/0.5.

mmol/L) was separately weighed for each of the formulation and transferred into Schlenck tubes, the monomer solutions were then added to the respective Schlenk tubes. The tubes were then degassed by three freeze−pump−thaw cycles and then heated to 90 °C. All polymerizations for the determination of C_{tr} were restricted to low conversions (<2%), with reaction mixtures being quenched by rapid cooling and the addition of hydroquinone prior to gravimetric determination of final conversions. Molecular weights were determined using SEC.

Results and Discussion

The choice of the initiator for the copolymerization is very briefly dealt with, followed by the determination of chain transfer constant (C_{tr}) for 1-octene in MMA. Then, the synthesis of the copolymers and comparison of the ATRP results with the conventional free radical systems will be discussed. The influence of the olefin during the copolymerization is highlighted. Furthermore, copolymer characterization using MALDI−TOF−MS is discussed. Also, the synthesis of block copolymer with clear insight into the macroinitiator efficiency is explained.

Choice of Initiator. The CuCl/PMDETA catalyst system was used in the copolymerization. PMDETA was selected because the catalyst complex is (i) highly active, leading to faster rates of polymerization (especially useful since a very nonreactive monomer like 1-octene was present), (ii) readily available, and (iii) cheap, and most importantly, (iv) the catalyst complex can be easily separated from the polymer. This is aided by the fact that a heterogeneous system was obtained when a nonpolar solvent (e.g., *p*-xylene, toluene) was employed for the polymerization. Now, since, the CuX/PMDETA (X = Cl, Br) is known to be a highly active catalyst system, more so with monomers such as MMA or in general methacrylates, with high observed propagation rate constants ($k_p^{obs} = k_p K_{eq}$; $K_{eq} \sim 10^{-7}-10^{-6}$ for MMA with PMDETA/CuBr),[14] the choice for the initiator is crucial to avoid slow initiation and possible side reactions.

Percec[15] and co-workers were the first to demonstrate the use of arenesulfonyl halides as universal initiators for heterogeneous and homogeneous metal-catalyzed living radical polymerization of styrene, methacrylates and acrylates. 2,2,2-Trichloroethanol (TCE) was used as an initiator, which resulted in a fast and nearly quantitative initiation of MMA using a CuCl/bpy catalyst system.[16] ATRP of MMA using a EBriB/CuCl led to a good control on molecular weight and narrow MMD.[17]

For the present work, the initiators employed were restricted to *p*-toluenesulfonyl chloride (pTsCl) and TCE. Table 2 details the results obtained for the homopolymerization of MMA using the selected initiators in a CuCl/PMDETA system.

The homopolymerizations were performed in 50 vol % *p*-xylene at 90 °C. The molar ratio of initiator to catalyst to ligand was chosen the same for both the entries 1 and 2, which enabled to compare the reactions. A typical semilogarithmic kinetic plot of the homopolymerization is shown in Figure 2. The linearity clearly indicated that there were a constant number of growing chains during the polymerization. The MM increased linearly with conversion (Figure 3) and the final PDI was ≤1.25. Though, the initiator efficiency in the case of pTsCl was only 50%, as compared to that of TCE of 80%, the initiator efficiency for the pTsCl can be improved by decreasing the copper(I) to initiator ratio (Table 5, entry 2).

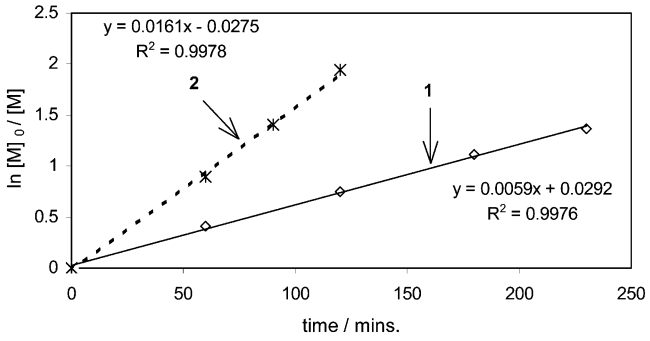

Figure 2. Plot of ln $[M]_0/[M]$ for the homopolymerization of MMA (Table 2).

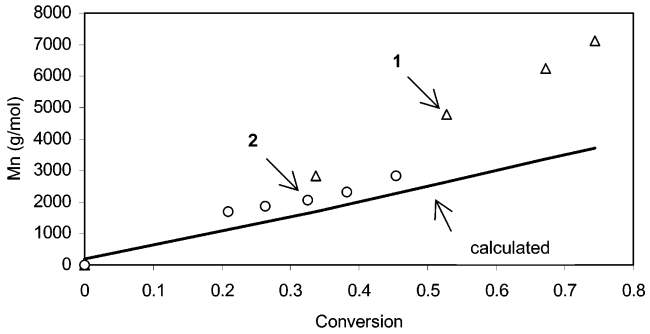

Figure 3. Plot of M_n vs conversion for the homopolymerizations (Table 2).

Determination of Chain Transfer Constant (C_{tr}) for 1-Octene in MMA. Since, higher α-olefins are known to act as chain transfer agents in radical polymerization,[10] it was interesting to determine the chain transfer constant for 1-octene during the radical polymerization of MMA. The activity of chain transfer is usually measured as the ratio between the transfer rate coefficient (k_{tr}) and the propagation rate coefficient (k_p). The Mayo method,[18] was employed, which expressed the reciprocal of the number-average degree of polymerization (DP_n), as a function of the rates of chain-growth and chain-termination;

$$\frac{1}{DP_n} = \frac{1}{DP_{no}} + C_{tr}\frac{[\text{1-octene}]}{[\text{MMA}]} \qquad (9)$$

where [1-octene] and [MMA] are the concentrations of the 1-octene and MMA respectively, and DP_{no} is the number-average degree of polymerization obtained in the absence of the transfer agent (in this case 1-octene).

Usually, the Mayo procedure involves the determination of DP_n at low conversion for a range of [1-octene]/[MMA] values and the plot of $1/DP_n$ vs [1-octene]/[MMA] should yield a straight line with slope C_{tr}. Values for the DP_n are commonly obtained by SEC. Since, the determination of number-average molar mass (M_n) by SEC, is very sensitive to baseline fluctuations, it is prudent to consider the weight-average molar mass (M_w), because it depends more on the high molar mass

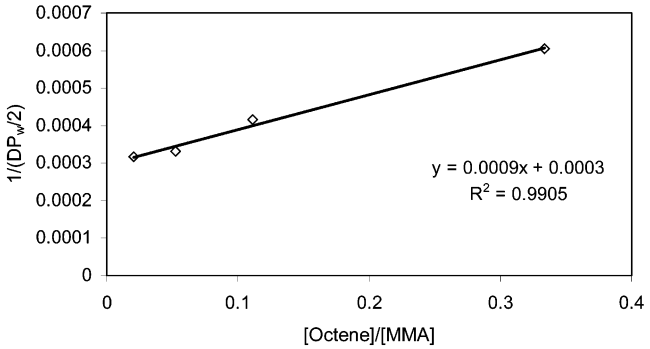

Figure 4. Plot of $1/(DP_w/2)$ vs [1-octene]/[MMA] ratios for determination of C_{tr}.

Table 3. C_{tr} Experiments

MMA (mol %)	1-octene (mol %)	% convn	M_w (g/mol)
100		1.1	6.4×10^5
98	2	1.1	6.3×10^5
95	5	1.0	6.0×10^5
90	10	0.8	4.8×10^5
75	25	0.6	3.3×10^5

region of the distribution, which is better defined. Assuming that $M_w/M_n = 2$ in a chain transfer dominated system at low conversions, the Mayo procedure can now be applied by plotting $1/(DP_w/2)$ vs [1-octene]/[MMA].[19,20]

The polymerizations were carried out in MMA at 90 °C for 5 min. A wide range of [MMA]/[1-octene] ratios were employed. Low initiator concentration was used ([Vazo 88] = 10 mmol/L), so that chain transfer and not bimolecular termination largely occurred as chain stopping events. The polymerizations were stopped at low conversion, that is, below 2%, so that the [MMA]/[1-octene] ratios were kept relatively constant, and thus, accurate C_{tr} values could be obtained.

Table 3 gives the different ratio of the [MMA]/[1-octene] employed and also the M_w obtained from SEC. M_w values shift to lower MM with increasing 1-octene concentrations, clearly indicating that 1-octene does act as a transfer agent in free radical polymerization. Also clear was that, as the mole percent of 1-octene increased in the monomer feed, the percent conversion decreased. This can be attributed to the fact that, more allylic radicals were obtained as a result of chain transfer, and these formed radicals were slow to reinitiate the polymerization. Hence, retardation in the rate of polymerization was obtained. Now, using eq 8, the value for the C_{tr} was obtained (Figure 4). The value for the C_{tr} was 9×10^{-4}. On comparison with the chain transfer to monomer value 0.1×10^{-4} for methyl methacrylate at 90 °C,[21] it turned out that the chain transfer constant to 1-octene is approximately 2 orders of magnitude larger.

MMA/1-Octene Copolymers Free radical copolymerization (FRP) initiated by AIBN and Vazo 88, and ATR copolymerization of MMA in the presence of 1-octene using TCE as initiator were examined as summarized in Table 4.

In Table 4, copolymerizations are listed at different comonomer ratios. Each of the comonomer ratios was polymerized under ATRP as well as under FRP conditions. A couple of observations can be made: (i) 1-octene does copolymerize via a radical mechanism. Homopolymerization of 1-octene was attempted in both FRP and ATRP, but no polymer was obtained. This is attributed to the fact that α-olefins undergo degradative chain

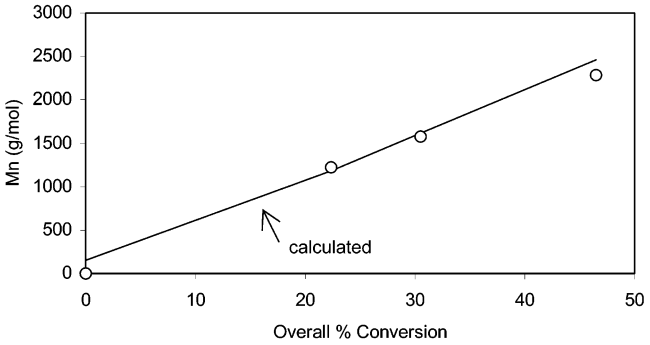

Figure 5. Plot of M_n vs overall percent conversion for entry 8 (Table 4).

Table 4. Copolymers of MMA/1-Octene (TCE Initiator)[a]

entry	f_{Oct}	fract convn	F_{Oct} [g]	M_n (g/mol)	PDI
1[b]		0.47		6.6×10^4	2.0
2[c]	0.25	0.73	0.06	1.8×10^4	1.9
3[d]	0.25	0.79	0.08	1.7×10^4	2.7
4[e]	0.25	0.73	0.06	4.6×10^3	1.2
5[f]	0.25	0.78	0.07	6.2×10^3	1.3
6[c]	0.50	0.48	0.16	1.0×10^4	2.0
7[d]	0.50	0.58	0.18	9.4×10^3	2.7
8[e]	0.50	0.47	0.19	2.3×10^3	1.3

[a] For all solution (co)polymerizations listed above, *p*-xylene was used as the solvent. Volume {solvent}/{monomer} = 1/0.5; reaction temperature = 90 °C; reaction time = 25 h. [b] FRP; initiator = Vazo88 (10 mmol/L); reaction time − 2 h. [c] FRP; initiator = AIBN (10 mmol/L). [d] FRP; initiator = Vazo88 (10 mmol/L). [e] ATRP; targeted M_n = 5000 g/mol; [TCE]:[CuCl]:[PMDETA] = 1:0.4:0.4. [f] ATRP; targeted M_n = 5000 g/mol; [TCE]:[CuCl]:[PMDETA] = 1:1:1. [g] Calculated from monomer conversions, obtained from GC measurements.

transfer of allylic hydrogens.[10] The stable allylic radical derived from the monomer is slow to reinitiate and prone to terminate. The presence of the formation of the stable allylic radical is further confirmed by electron spin resonance.[22] (ii) The copolymerization under FRP conditions, show relatively low MM as compared to the MMA homopolymerization under same conditions (*compare entry 1 with entries 2, 3, 6 and 7*). Broad MMD was obtained for all FRP systems. In this paper itself, the tendency for 1-octene to behave as a chain transfer agent under FRP conditions was reported. The value for the C_{tr} was found to be 9×10^{-4}, in the case of MMA systems. (iii) The experimentally determined MM in the case of polymerizations under ATRP conditions coincide nicely with the calculated values (Figure 5). The linearity clearly indicated that there were a constant number of growing chains during the polymerization. (iv) More interestingly, narrow MMD were obtained in the ATRP experiments, which points at ordinary ATRP behavior, i.e., no peculiarities caused by the incorporation of 1-octene. (v) As the mole percent of the α-olefin was increased in the monomer feed, its incorporation was higher in the copolymer (*compare entries 3 and 6, 4 and 7, and 5 and 8*). This is to be expected, since the probability of the 1-octene getting incorporated within the polymer chain during polymerization was higher. (vi) Higher mole percent of the 1-octene in the monomer feed resulted in lower overall percent conversion coupled with lower MM (*compare entries 3 and 6, 4 and 7, and 5 and 8*). Two effects can cause these phenomena. Because of composition drift, the fraction 1-octene in the remaining monomer increases, which leads to a decrease in average propagation rate constant. When the fraction 1-octene increases, the probability of end-capping a

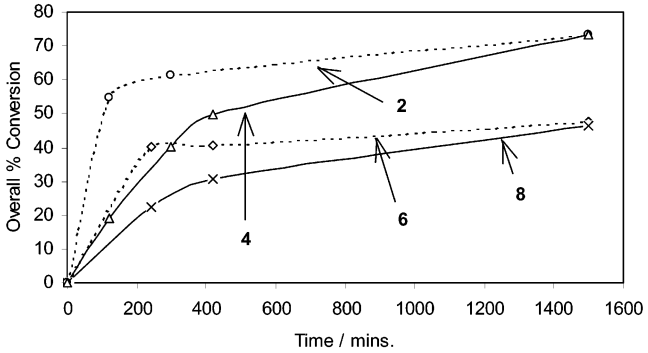

Figure 6. Plot of overall percent conversion vs time for the described copolymerizations. For the labels, refer to Table 4.

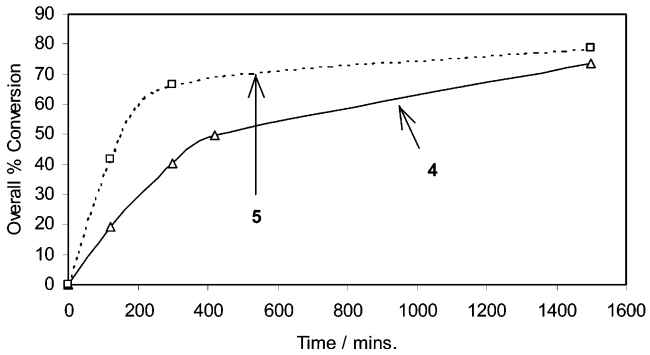

Figure 7. Influence of [Cu(I)] on conversion. Plot of overall percent conversion vs time for the described copolymerizations. For the labels, refer to Table 4.

1-octene moiety at the chain end with a bromide increases. When this happens the chain will be virtually inactive as we learned from model experiments. Thus, increasing the mole percent of α-olefin in the monomer feed decreased the overall percent conversion (Figure 6). (vii) Varying the Cu(I) to initiator does influence the reaction kinetics (*compare entries 4 and 5*). A higher Cu(I) concentration leads to an increase in the initial radical concentration and in turn to slightly faster polymerization rates (Figure 7). But as observed, it does not alter the final amount of 1-octene incorporated. Now, it is known that $k_t \propto [R^*]^2$ and $k_p \propto [R^*]$, where k_t and k_p are the rate coefficient of termination and propagation, respectively. [R*] stands for radical concentration. Hence, a higher initial radical concentration, would lead to some portion of the initiator radicals being lost due to bimolecular termination at the onset of the polymerization and hence to a lower initiator efficiency.

The copolymerizations were also performed using pTsCl as initiator, since for the homopolymerization of MMA narrower MMDs were obtained (Table 2). The trend obtained for the copolymerization from Table 5, was comparable to that observed in Table 4. In this table, narrow MMD were obtained in the ATRP experiments, which points at ordinary ATRP behavior.

The only exception is entry 3, where the MMD was relatively broad and very low molecular weight was obtained. The plot of overall percent conversion vs time (Figure 8) indicated that, in the presence of higher 1-octene in the monomer feed, a drastic decrease in the overall percent conversion was observed. This was coupled with the fact that, there was no linear increase in the molecular weight with conversion (Figure 9), clearly indicating that the reaction was not controlled.

The important difference between alkyl halides and arylsulfonyl halides arises in the initiation mechanism

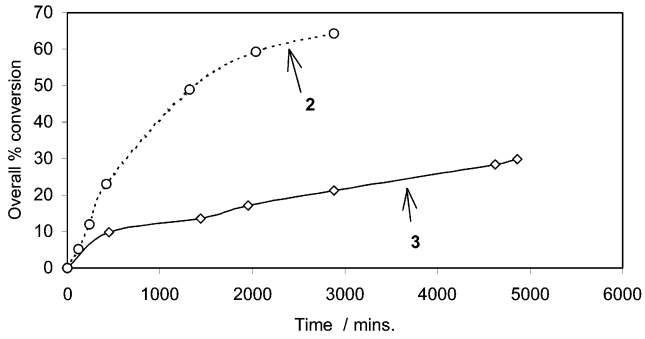

Figure 8. Plot of overall percent conversion vs time. For the labels refer to Table 5.

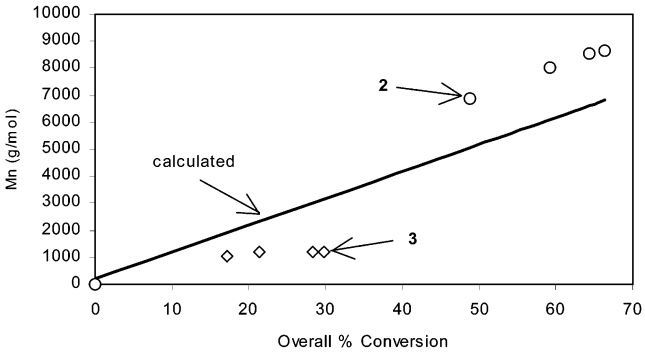

Figure 9. Plot of M_n vs overall percent conversion. For the labels refer to Table 5.

Table 5. Copolymers of MMA and 1-Octene (pTsCl Initiator)[a]

entry	f_{Oct}	fract convn	F_{Oct}[e]	M_n (g/mol)	PDI
1[b]	0.10	0.80	0.02	7.4×10^3	1.1
2[c]	0.25	0.66	0.07	8.6×10^3	1.1
3[d]	0.50	0.30	0.26	1.2×10^3	1.3

[a] For all solution ATR(co)polymerizations listed above, *p*-xylene was used as the solvent. Volume {solvent}/{monomer} − 1/0.5; reaction temperature − 90 °C. [b] Targeted M_n = 5000 g/mol; [pTsCl]:[CuCl]:[PMDETA] = 1:0.5:0.5; reaction time = 9 h 30 min. [c] Targeted M_n = 10000 g/mol; [pTsCl]:[CuCl]:[HMTETA] = 1:0.285:0.285; reaction time = 70 h. [c] Targeted M_n = 10000 g/mol; [pTsCl]:[CuCl]:[HMTETA] = 1:0.285:0.285; reaction time = 81 h. [d] Calculated from monomer conversions, obtained from GC measurements.

Scheme 2. Initiation Mechanism for Substituted Phenylsulfonyl Chlorides[23]

$$R{-}X + Cu^{I}X/L \underset{k_{-i1}}{\overset{k_{i1}}{\rightleftharpoons}} R^* + Cu^{II}X_2/L \quad (10)$$

$$R^* + M \underset{k_{-i2}}{\overset{k_{i2}}{\rightleftharpoons}} P_1^* \quad (11)$$

$$P_1^* + Cu^{II}X_2/L \underset{k_{-i3}}{\overset{k_{i3}}{\rightleftharpoons}} P_1{-}X + Cu^{I}X/L \quad (12)$$

(Scheme 2, eqs 10−12).[23] The arylsulfonyl halides undergo faster reduction to the corresponding sulfonyl radical, which in turn results in the faster addition of the sulfonyl radicals to the monomer. This addition is reversible, and the equilibrium of the reversible addition is determined by the nature of the substituent attached to the monomer and its ability to stabilize the resulting radical. As in the present case, when there is more 1-octene in the monomer feed (Table 5, entry 3), then the probability of 1-octene adding to the sulfonyl radical in the initiation step is increased. If that occurs, then

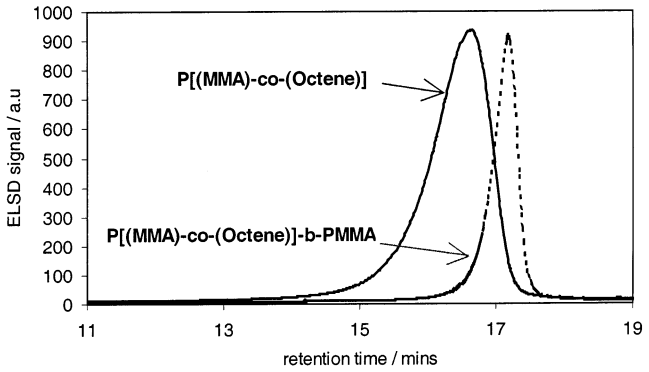

Figure 10. GPEC traces of the macroinitiator and the block copolymer, respectively.

Table 6. Block Copolymer[a]

entry	M:I:Cu:L	reacn time (h)	fract convn	theor M_n (g/mol)[b]	exptl M_n (g/mol)[c]	PDI
1	77:1:1:1	11	0.64	6.4×10^3	5.5×10^3	1.5

[a] Volume {solvent}/{monomer} = 1/0.5. Targeted molecular weight = 10000 g/mol. [b] $[((([MMA]_0 * \text{conversion})/[\text{macroinitiator}]_0)\text{-}M_{MMA}] + M_{\text{macroinitiator}}$. [c] From SEC analysis, using universal calibration for PMMA with PS standards.

reinitaition of this monoadduct (with the 1-octene as the terminal group), is very unlikely, since there are no substituent groups in the 1-octene to stabilize the obtained radical. Hence, the equilibrium is shifted to the dormant side. Work within our group on activation rate parameters using a 1-octene-type alkyl halide as a model compound resulted in no initiation. A more detailed paper entailing the results is currently under preparation. Thus, the result obtained for entry 3 can be explained due to the addition of the sulfonyl radicals to 1-octene, which in turn do not reinitiate the polymerization.

ATRP Initiated by P[(MMA)-*co*-(1-octene)]. Chain Extension with MMA. The synthesized copolymer (Table 4, entry 5) comprising 19 mol % of 1-octene in the copolymer was used as the macroinitiator for the block copolymerization. The resulting molecular weight and polydispersity was as summarized in Table 6. The living character of the copolymer was demonstrated by chain extension with MMA. High-performance liquid chromatography was employed for selective separation. It has been used previously for selective separation and characterization of block and random copolymers.[24] In this paper, the term gradient polymer elution chromtagraphy (GPEC) is used.[25] In GPEC, separation of the polymers is based on differences in column interactions, as in the case of isocractic chromatography, but also depends on precipitation and redissolution mechanisms as the eluent composition changes gradually in time. Hence, it is possible to separate polymers depending on molar mass, chemical composition and chain(-end) functionality. In the current study, normal phase GPEC with THF and *n*-heptane as eluent was employed. The gradient used is shown in Table 1. The GPEC trace in Figure 10 clearly indicated well-resolved peaks from the macroinitiator and the block copolymer. The shift of the block polymer peak from the macroinitiator peak was clear evidence for the block copolymer formation. The difference in the elution behavior was a direct indication of chemical composition difference between the macroinitiator and the block copolymer. The clear shift of the block copolymer peak to higher retention time, also indicated the high macroinitiator efficiency, which is characteristic of a living polymerization. This was coupled with the fact that, there was a reasonable match between the theoretical and experimentally determined molecular weights.

Polymer Characterization. The formation of the copolymer was established using the matrix assisted laser desorption/ionization−time-of-flight−mass spectrometry (MALDI−TOF−MS). Differential scanning calorimetry (DSC) was also employed to identify the difference in glass transition temperature (T_g) between the homopolymer of MMA and the formed copolymer.

Figure 11 depicted the MALDI−TOF−MS spectrum for the MMA/1-octene copolymer (Table 5, entry 2). The copolymer obtained using pTsCl as initiator was only investigated, primarily due to the relative ease in peak assignment. The overlap of several signal distributions was clearly visible. This was typical for the resolved mass distributions of a copolymer, since copolymers have, in comparison with homopolymers, two types of heterogeneity. Like homopolymers, they have the heterogeneity in the degree of polymerization, corresponding to a distribution of the chain length. Additionally, there is the heterogeneity of the chemical composition.

Figure 12 is an expansion of a selected portion of the spectrum shown in Figure 11. The peak assignments were made using the following strategies: (i) comparison with the MMA homopolymer spectrum; (ii) comparison of the observed masses with those theoretically calculated. The polymer chains were cationized with potassium, therefore were detected at a *m*/*z* value 39

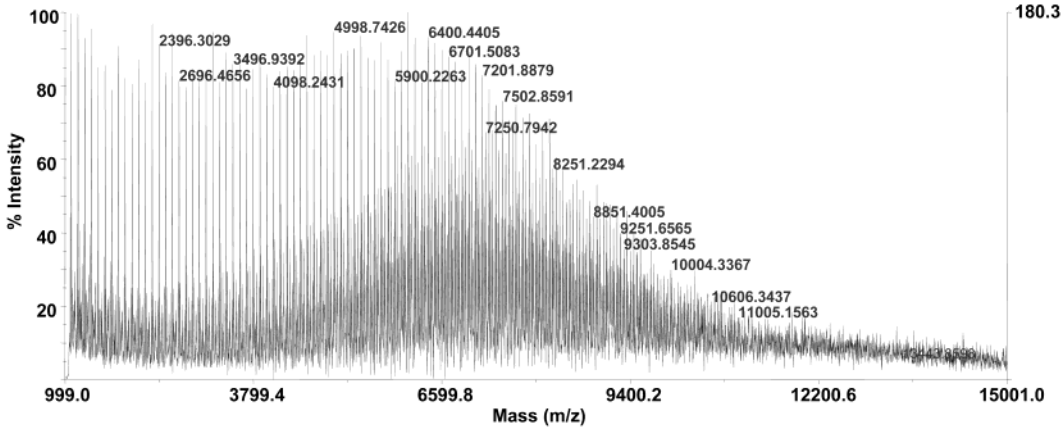

Figure 11. MALDI−TOF−MS spectrum for MMA/Oct copolymer (Table 5, entry 2). [Spectrum acquired in the reflector mode, matrix = DCTB (*trans*-2-[3-(4-*tert*-butylphenyl)-2-methyl-2-propenylidene]malononitrile).]

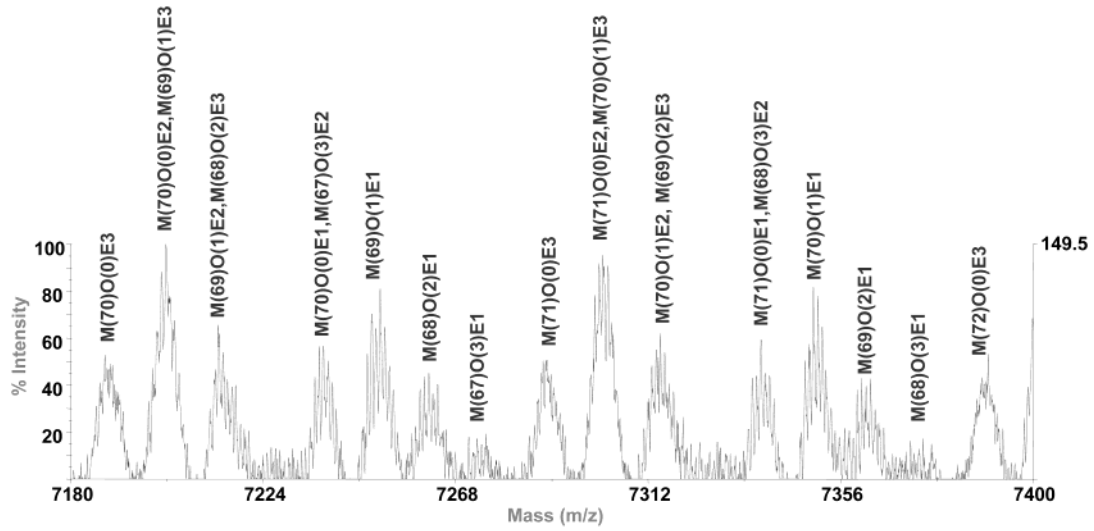

Figure 12. MALDI−TOF−MS spectrum for MMA/Oct copolymer (Table 5, entry 2). [Spectrum acquired in the reflector mode, matrix = DCTB (*trans*-2-[3-(4-*tert*-butylphenyl)-2-methyl-2-propenylidene]malononitrile).]

Da above the theoretically calculated mass. All the polymer chains were assigned to various chemical compositions, constituting of varying MMA (M) and 1-octene (O) units. Interestingly, all copolymer chains can be divided into having three pairs of end groups (E1, E2, E3).

Usually, the detected signals after subtraction of the mass of the cationization reagent, should be in agreement with the expected masses of the copolymer chains, which can be calculated according to eq I. End group E1 was assigned to eq I.

$$M_{copo} = 155.19 + [(m \times 100.12) + (n \times 112.21)] + 35.45 \quad \text{(I)}$$

where 155.19 and 35.45 are the average masses of the end groups from the initiator fragment and the chloride respectively (since pTsCl was used as the ATRP initiator), 100.12 and 112.21 are the average masses of the MMA and 1-Octene repeating units, respectively, and *m* and *n* are the numbers of the monomers in the chain.

In MALDI−TOF−MS, during ionization (in the employed range of laser intensity) it is observed that some of the terminal halide gets dislodged. Other groups have also reported the loss of the halide during MALDI−TOF−MS analysis.[26] Recently, it was reported that during MALDI−TOF−MS of PMMA synthesized by ATRP, a dissociation reaction occurred to form CH_3Br, preceded by cyclization of the terminal two repeat units of the polymer chain, giving rise to a lactone end group.[27]

End group E2 arises due to the loss of the terminal halide. To explain end group E2, eq II can be employed, which is a slight modification to eq I. The difference between the two equations is that eq I accounts for the Cl at the chain end and eq II does not.

$$M_{copo} = 155.19 + [(m \times 100.12) + (n \times 112.21)] \quad \text{(II)}$$

where 155.19 is the average mass of the end group from the initiator fragment, 100.12 and 112.21 are the average masses of the MMA and 1-Octene repeating units, respectively, and *m* and *n* are the numbers of the monomers in the chain.

End groups E3 is assigned to the polymer chains having a lactone group on one end and the *p*-toluenesulfonyl initiator fragment on the other end (eq III). The lactone end group, which as explained, resulted due to loss of CH_3Cl preceded by cyclization of the terminal two repeat units of the polymer chain.

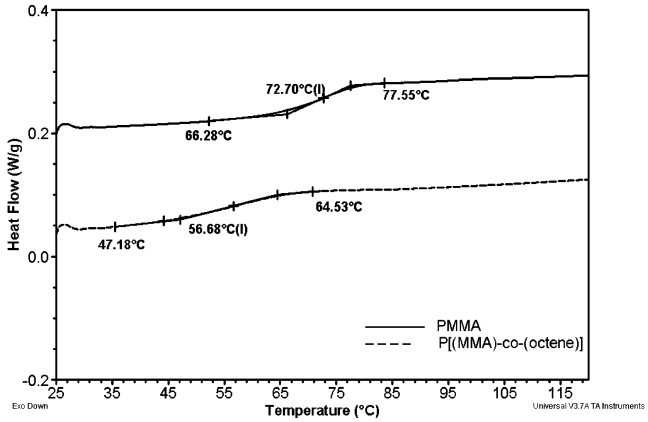

Figure 13. DSC curves comparing the difference in the obtained T_g for the homopolymer of PMMA and the copolymer of P[(MMA)-*co*-(1-octene)].

$$M_{copo} = 155.19 + [(m \times 100.12) + (n \times 112.21)] + 185.2 \quad \text{(III)}$$

where 155.19 and 185.2 are the average masses of the end groups from the initiator fragment and the lactone ring respectively, 100.12 and 112.21 are the average masses of the MMA and 1-octene repeating units, respectively, and *m* and *n* are the numbers of the monomers in the chain.

The important point in Figure 12 is that most polymer chains contain at least one 1-octene unit, which was clear evidence that the 1-octene became incorporated in the chain during the polymerization.

DSC measurements were performed on the PMMA homopolymer (Table 2, entry 2) and the poly[(MMA)]-*co*-(1-octene)] copolymer (Table 4, entry 8). Now, since the molecular weight of the two polymers under consideration was similar, coupled with the fact that the end groups for the two polymers were the same (since the same initiator/catalyst system was employed for both the polymerizations), it was possible to compare the obtained glass transition temperatures (T_g). Now

from the literature,[28] the T_g reported for the homopolymers of MMA and 1-octene was +100 and −41 °C, respectively. Since, the molecular weights of the polymers currently under consideration were much lower than those employed in the literature, the T_g values will not be the same. However, the important point is that if 1-octene gets incorporated in the polymer, the T_g would be expected to be lower for the copolymer, as compared to that for the homopolymer of MMA. It was very clear from Figure 13 that the T_g decreased by around 16 °C for the copolymer. This was further evidence that the 1-octene became incorporated during the polymerization.

Conclusion

The atom transfer radical (co)polymerization (ATRP) of methyl methacryalte (MMA) with 1-octene was investigated. The importance of the initiator employed and the initiation mechanism in the presence of the olefin is highlighted. 2,2,2-trichoroethanol (TCE) and *p*-toluenesulfonyl chloride (pTsCl) were efficient initiators due to higher initiation rates compared to the propagation rates. However, during copolymerization, uncontrolled polymerization occurred when pTsCl was employed in the presence of higher mol % of 1-octene in the monomer feed. This could be explained by the difference in the initiation mechanism between TCE and pTsCl.

Well-controlled copolymers constituting almost 20 mol % of 1-octene were obtained using TCE as initiator. Narrow molar mass distribution (MMD) were obtained in the ATRP experiments, which points at ordinary ATRP behavior, i.e., no peculiarities caused by the incorporation of 1-octene**.** The comparable free radical (co)polymerizations (FRP) resulted in broad MMD. An increased fraction of the olefin in the monomer feed, leads to an increased level of incorporation of the olefin in the copolymer, at the expense of the overall percent conversion.

The formation of the copolymer was established using the matrix assisted laser desorption/ionization−time-of-flight−mass spectrometry (MALDI−TOF−MS). Differential scanning calorimetry (DSC) was also employed to identify the difference in glass transition temperature (T_g) between the homopolymer of MMA and the formed copolymer. Evident from the MALDI spectra was that, most polymer chains contained at least one 1-octene unit. The glass transition temperature of the copolymer was 16 °C lower than that for the homopolymer of MMA. Both results were clearly indicative of the fact that 1-octene was incorporated during the polymerization.

Block copolymer was synthesized using P[(MMA)-*co*-(1-octene)] as the macroinitiator and further characterized using gradient polymer elution chromatography (GPEC). The shift in the retention time between the macroinitiator and the formed block clearly indicated the existence of the block copolymer structure and also confirmed the high macroinitiator efficiency.

Acknowledgment. The authors of this paper would like to thank the Dutch Polymer Institute for financial support of this research. Mr. Wieb Kingma, Mr. Bastiaan Staal, and Mr. Wouter Gerritsen are acknowledged for the SEC, MALDI−TOF−MS, and DSC analysis, respectively. Thanks are due to Dr. Michael Monteiro, Dr. Sreepadaraj Karanam, and Dr. Auke Snijder for fruitful discussions during the course of this work.

References and Notes

(1) Padwa, A. R. *Prog. Polym. Sci.* **1989**, *14*, 811.
(2) *Functional Polymers: Modern Synthetic Methods and Novel Structures*; Patil, A. O., Schulz, D. N., Novak, B. M., Eds.; ACS Symposium Series 704; American Chemical Society: Washington, DC, 1998.
(3) Johnson, L. K.; Killian, C. M.; Brookhart, M. *J. Am. Chem. Soc.* **1995**, *117*, 6414. Killian, C. M.; Temple, D. J.; Johnson, L. K.; Brookhart, M. *J. Am. Chem. Soc.* **1996**, *118*, 11664.
(4) Johnson, L. K.; Mecking, S.; Brookhart, M. *J. Am. Chem. Soc.* **1996**, *118*, 267. Mecking, S.; Johnson, L. K.; Wang, L.; Brookhart, M. *J. Am. Chem. Soc.* **1998**, *120*, 888.
(5) Wang, C.; Friedrich, S.; Younkin, T. R.; Li, R. T.; Grubbs, R. H.; Bansleben, D. A.; Day, M. W. *Organometallics* **1998**, *17*, 3149.
(6) Yasuda, H.; Furo, M.; Yamamoto, H. *Macromolecules* **1992**, *25*, 5115. Yasuda, H.; Ihara, E. *Macromol. Chem. Phys.* **1995**, *196*, 2417.
(7) Ittel, S. D.; Johnson, L. K.; Brookhart, M. *Chem. Rev.* **2000**, *100*, 1169. Boffa, L. S.; Novak, B. M. *Chem. Rev.* **2000**, *100*, 1479.
(8) Tian, G.; Boone, H. W.; Novak, B. M. *Macromolecules* **2001**, *34*, 7656.
(9) Liu, S.; Elyashiv, S.; Sen, A. *J. Am. Chem. Soc.* **2001**, *123*, 12738.
(10) Rudin, A. *The Elements of Polymer Science and Engineering*, 2nd ed.; Academic Press, 1999; p 218.
(11) Kato, M.; Kamigaito, M.; Sawamoto, M.; Higashimura, T. *Macromolecules* **1995**, *28*, 1721.
(12) Wang, J. S.; Matyjaszewski, K. *Macromolecules* **1995**, *28*, 7901.
(13) Beuermann, S.; Paquet, D. A., Jr.; McMinn, J. H.; Hutchinson, R. A. *Macromolecules* **1996**, *29*, 4206.
(14) Snijder, A.; Klumperman, B.; van der Linde, R. *Macromolecules* **2002**, *35*, 4785.
(15) Percec, V.; Barboiu, B. *Macromolecules* **1995**, *28*, 7970.
(16) Destarac, M.; Matyjaszewski, K.; Boutevin, B. *Macromol. Chem. Phys.* **2000**, *201*, 265.
(17) Matyjaszewski, K.; Wang, J. L.; Grimaud, T.; Shipp, D. A. *Macromolecules* **1998**, *31*, 1527.
(18) Mayo, F. R. *J. Am. Chem. Soc.* **1943**, *65*, 2324.
(19) Moad, G.; Moad, C. L. *Macromolecules* **1996**, *29*, 7727.
(20) Heuts, J. P. A.; Kukuj, D.; Forster, D. J.; Davis, T. P. *Macromolecules* **1998**, *31*, 2894.
(21) Ueda, A.; Nagai, S. In *Polymer Handbook*, 4th ed.; Brandrup, A., Immergut, E. H., Grulke, E. A., Eds.; John Wiley and Sons: New York, 1999, Section II.
(22) Unpublished results. Work done in collaboration with Kajiwara, A.
(23) Percec, V.; Barboiu, B.; Kim, H.-J. *J. Am. Chem. Soc.* **1998**, *120*, 305.
(24) Katz, E.; Eksteen, R.; Schoenmakers, P.; Miller, N. *Handbook of HPLC*; Marcel Dekker: New York, 1979. Karanam, S.; Goossens, H.; Klumperman, B.; Lemstra, P. *Macromolecules* **2003**, *36*, 3051.
(25) Philipsen, H. J. A.; De Cooker, M. R.; Claessens, H. A.; Klumperman, B.; German, A. L. *J. Chromatogr. A* **1997**, *761*, 147.
(26) Matyjaszewski, K.; Nakagawa, Y.; Jasieczeck, C. B. *Macromolecules* **1998**, *31*, 1535. Coessens, V.; Matyjaszewski, K. *J. Macromol. Sci.—Pure Appl. Chem.* **1999**, *A36*, 653. Coessens, V.; Matyjaszewski, K. *J. Macromol. Sci.—Pure Appl. Chem.* **1999**, *A36*, 667.
(27) Borman, C. D.; Jackson, A. T.; Bunn, A.; Cutter, A. L.; Irvine, D. J. *Polymer* **2000**, *41*, 6015.
(28) Andrews, R. J.; Grulke, E. A. In *Polymer Handbook*, 4th ed.; Brandrup, A., Immergut, E. H., Grulke, E. A., Eds.; John Wiley and Sons: New York 1999; Section VI.

MA035231F